

## An Evaluation of Free- and Fixed-Vane Flowmeters with Curved- and Flat-Bladed Savonius Rotors

ANTONY JOSEPH AND EHRLICH DESA

*Marine Instrumentation Division, National Institute of Oceanography, Dona Paula, India*

(Manuscript received 22 January 1993, in final form 3 August 1993)

### ABSTRACT

Speed and direction performances of flowmeters, designed by the authors for in-house use, employing an Aanderaa-type curved-bladed Savonius rotor and a free vane and an Aanderaa-type flat-bladed Savonius rotor and a fixed vane, are discussed. It has been observed that accuracy, linearity, and tilt response of a meter using the Aanderaa curved-bladed rotor is superior to those of a meter using the Aanderaa flat-bladed rotor. Analysis showed that the azimuth response of a flowmeter is affected by the presence of support rods surrounding its rotor. The change in azimuth response arises from flow pattern modifications in the vicinity of the rotor, imposed by the changes in the horizontal angle of the support rods of the rotor relative to the flow streamlines. While the use of two support rods may be suitable for a fixed-vane system, it is undesirable for a free-vane system where the meter's orientation with respect to the flow direction is not defined. Flow direction calibration results indicated that a fixed-vane system exhibits superior direction performance compared to a free-vane system. The comparatively poor direction performance of the free-vane system stems from the poor coupling to the "vane-follower" magnet from the external vane.

### 1. Introduction

Eulerian flowmeters employ a wide range of sensors such as the Savonius rotor, unidirectional impellers, bidirectional propeller pairs, electromagnetic sensors, acoustic travel-time difference sensors, and acoustic Doppler sensors. In some specialized situations, such as measurements of turbulence and very small flows, thermal and laser Doppler sensors are also used. While all these sensors have varying degrees of merits and demerits, the choice of a particular type of sensor often depends on the type of study to be undertaken. A flowmeter intended for measurements in estuaries and inlets must be able to measure flows as large as  $300 \text{ cm s}^{-1}$  or more. Because tidal variations in estuaries introduce variations in salinity and temperature, and some locations have large sediment concentrations, the flowmeter must also be insensitive to these effects. The Savonius rotor's insensitivity to variations in surrounding environmental conditions is its noteworthy feature, making it suitable for flow measurements in estuaries and inlets. Because Aanderaa-type curved-bladed and flat-bladed rotors were readily available, tethered flowmeters incorporating these two types of rotors were used in our design. The flowmeter with the curved-bladed rotor incorporated a free-vane assembly (Fig. 1a) and that with the flat-bladed rotor assembly incorporated a fixed vane (Fig. 1b) for measurement of

flow direction. The primary goal of the present work is the evaluation of free- and fixed-vane flowmeters incorporating curved- and flat-bladed Savonius rotors.

### 2. Description of instruments

The flowmeters evaluated in this paper consisted of an in-water unit for detection of flow speed and direction, and a deck-based terminal to view the data. Flow speed was detected by means of a Savonius rotor whose number of rotations in unit time was directly proportional to the flow. The Savonius rotor was supported between two flat stainless-steel (SS) plates mounted 9 cm away from the midpoint of the rotor. Height of the blades of the curved-bladed rotor was 6.5 cm and that of the flat-bladed rotor 5 cm. The rotor was free to rotate between two Teflon bearings embedded in two SS rods mounted on these two plates. The speed detection assembly consisting of a follower magnet, reed switch, and associated signal conditioning electronics was mounted in a pressure-proof SS housing of the in-water unit. While the curved-bladed rotor had two support rods immediately surrounding it, the miniature flat-bladed rotor with a "paddle-wheel" arrangement had a semicylindrical cover and three support rods immediately surrounding it. While two rods formed part of the semicylindrical cover, the third support rod was placed diametrically opposite to the semicylindrical cover.

In the free-vane flowmeter (Fig. 1a), a miniature wedge-shaped vane (Fig. 2a), with a bar magnet con-

*Corresponding author address:* Dr. Antony Joseph, National Institute of Oceanography, Dona Paula, Goa-403 004, India.

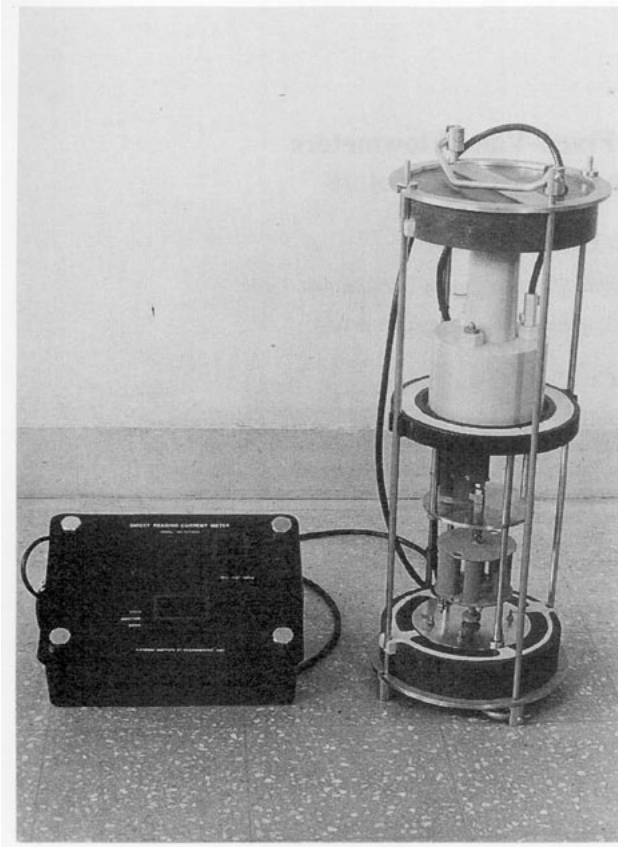
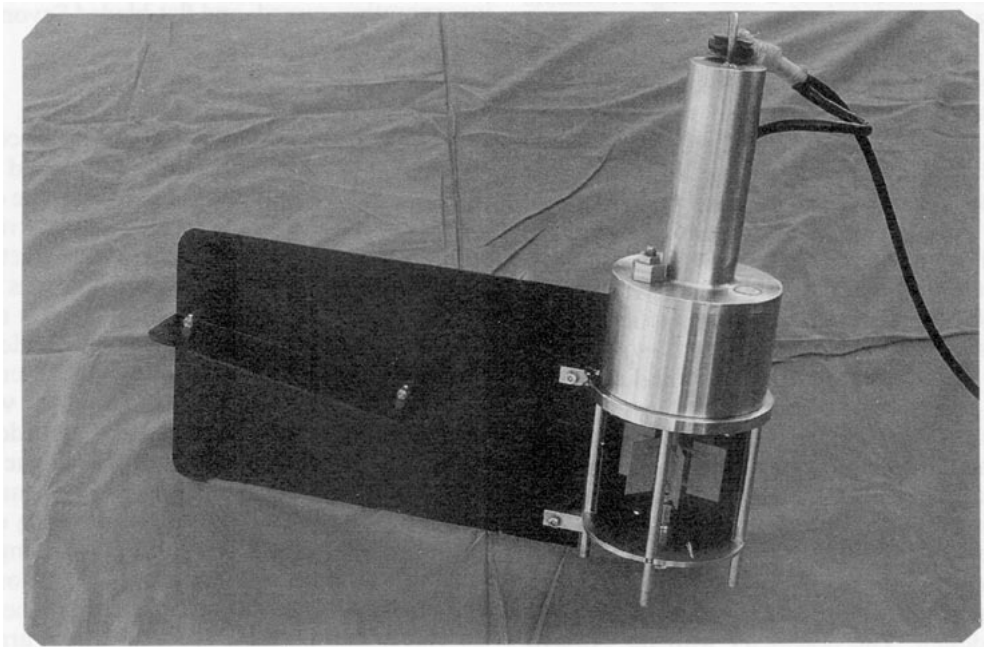


FIG. 1. (a) Flowmeter with curved-bladed Savonius rotor and free vane. (b) Flowmeter with flat-bladed rotor assembly and fixed vane.



sealed in its top end, was axially mounted between two circular plates above the rotor. This neutrally buoyant vane, designed as an open wedge to reduce the effect of jitter arising from turbulent flow, was free to rotate

between two Teflon bearings about the instrument's axis and within the instrument frame. The vane and a magnetic north-seeking compass formed the direction sensors. The vane magnetically turned the wiper of a

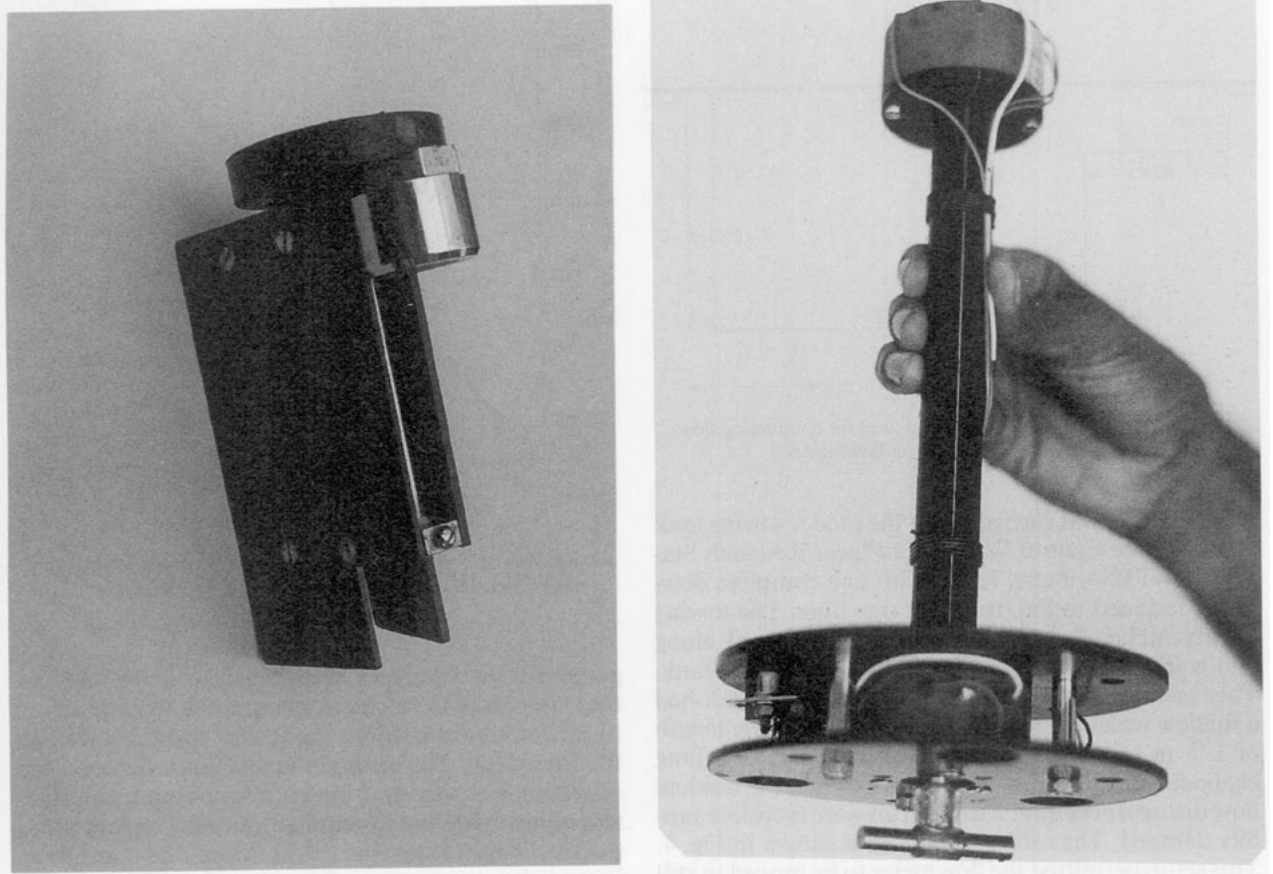


FIG. 2. (a) Open wedge-shaped miniature free vane used in the flowmeter of Fig. 1a. (b) Magnetic compass (top) and cylindrical bar magnet (bottom) rigidly mounted on the stud of a precision circular potentiometer (located between two circular plates), which magnetically couples to the free vane in panel (a).

low-torque single-turn circular potentiometer to the direction of water flow, while the north-seeking compass related the orientation of the vane to the magnetic north. The magnetic compass was kept sufficiently distant from the magnetic coupling arrangements of the vane. Immediately above the free vane, a pressure-proof casing housed the precision potentiometer and the magnetic compass (Fig. 2b). The whole arrangement was locked within an SS frame consisting of four rods and two annular rings. This frame could be used to carry a ballast to weight the flowmeter in high velocity fields. The design aspects of the free-vane system have been reported by Joseph et al. (1986). In the fixed-vane flowmeter (Fig. 1b) a long vane, rigidly fixed to one side of the in-water unit, and a magnetic north-seeking compass directly aligned with the vane formed the flow direction sensors. Correct alignment was achieved by pointing the "zero" of the magnetic compass to the axis of the vane. The vane and the in-water unit aligned in the direction of flow; therefore, the magnetic compass reading was a direct measure of the direction of water flow.

The two types of flowmeters mentioned above incorporated similar terminals to view data on seven-segment LED (light-emitting diode) displays. A simple technique used for display of data reduced hardware and required a smaller software overhead (Joseph 1987). The deck-based data terminal essentially consisted of a single printed circuit card mounted inside a weather-proof casing. A Perspex lid with rubber sealing served as the front panel. A black neoprene rubber sunhood, with a slanting black rubber tube provided with a red filter, mounted over the Perspex closing lid provided readability of the displayed data during daytime. A connector at one side of the data terminal allowed its decoupling from the in-water unit when the instrument was not in use, or when being transported.

### 3. Flow speed calibration

Calibration is the determination of the sensor's response to steady-state relative motion of water past the sensor. The calibration relation is a best fit of one or more linear segments over the range of interest, expressed as an intercept and slope (Dean 1985).

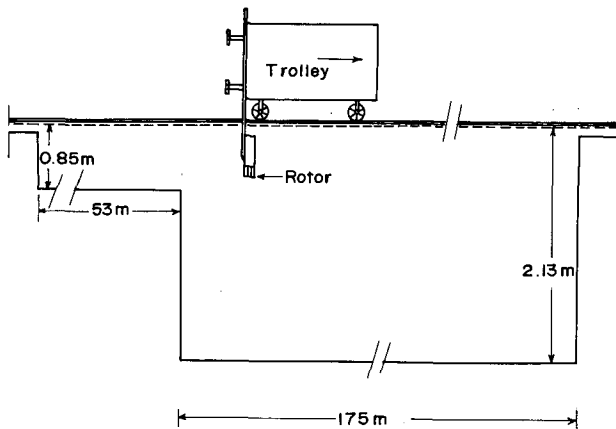


FIG. 3. Tow tank and trolley facility used for conducting flow evaluation experiments on flowmeters.

Calibration was carried out at the indoor towing tank facility at the Central Water and Power Research Station (CWPRS), Pune, India, with one complete flowmeter fastened to the trolley, at one time. The towing facility included a towed carriage that moved along two tracks built on the edges of a rectangular tank. This carriage supported the flowmeter. The tank had a shallow water length of 53 m and a deep water length of 175 m (see Fig. 3). This tank was part of a long channel extending from a nearby dam, and the residual flow disturbances after a trolley run were therefore rapidly damped. The calibration setup is shown in Fig. 4. This setup permitted the flowmeter to be moved in still water along the center of the tank with minimal flow disturbances. In conformity with conventional flow calibration procedure, the flowmeter was maintained normal to the trolley track. The flow calibration data and calibration relations for a curved bladed system, for the orientation shown, is given in Fig. 5. Data for Fig. 5 is shown in Table 1.

4. Evaluation of flow speed performance

Instrument parameters such as accuracy and linearity were deduced from least-squares-fitted calibration

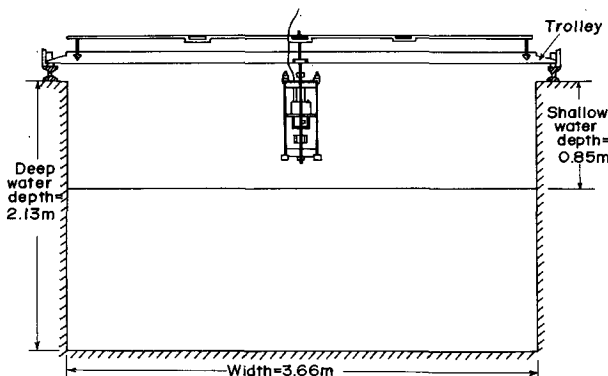


FIG. 4. Flow calibration setup.

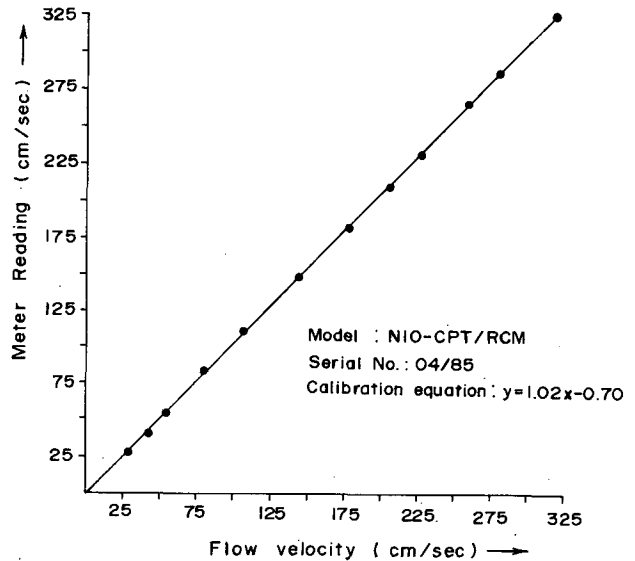


FIG. 5. Flow calibration relation for a typical curved-bladed rotor meter (Fig. 1a). Flow calibration data are given in Table 1.

graphs for the two types of systems. Accuracy refers to the closeness of the instrument output to the true value. In flowmeter calibration, the trolley speed is taken as the true value. The error is the difference between the instrument output and the corresponding true value, taken positive if the instrument output is greater than the true value (Doebelin 1983). More often, accuracy is quoted as a percentage figure based on the full-scale reading of the instrument. Because the instruments have been calibrated, at discrete steps of  $40 \text{ cm s}^{-1}$ , to a towing speed of  $300 \text{ cm s}^{-1}$ , the full scale has been specified as  $300 \text{ cm s}^{-1}$ . It is entirely possible, however, to operate at much higher flow speeds though calibration data is not available (Joseph and Desa 1992). Linearity is a specification relating to the degree of conformity of an instrument's calibration graph to the least-squares-fitted straight line behavior. The linearity

TABLE 1. Data for Fig. 5.

Flow velocity ( $\text{cm s}^{-1}$ ) (x)	Meter reading ( $\text{cm s}^{-1}$ ) (y)
29.07	28.00
42.63	41.06
54.97	54.50
80.92	84.00
107.14	111.00
145.45	149.00
179.64	182.00
208.09	211.00
229.50	232.00
260.67	267.00
283.33	287.00
320.86	327.00

is a measure of the deviation of the calibration points from this straight line. Deviation from linearity is the difference between the meter output and the corresponding least-squares-fitted value, taken positive if the instrument output is greater than the corresponding least-squares-fitted value (Doebelin 1983). Linearity is usually expressed as a percent of the full-scale reading (300 cm s<sup>-1</sup> in the present case).

The percentage flow accuracy and linearity of the curved-bladed system were within 2% and 1.25%, respectively. It has been observed that accuracy and linearity of both systems varied over the range of flow velocity.

In the range 10–160 cm s<sup>-1</sup>, accuracy of the curved-bladed meter varied from -1.25% to +1.50%, and in the range 161–300 cm s<sup>-1</sup> its accuracy lay within -1% and +2%. In the range 10–260 cm s<sup>-1</sup>, the percentage linearity of the curved-bladed system varied from -0.5% to +1%. Above 260 cm s<sup>-1</sup>, the curved-bladed system's linearity varied from -0.5% to +1.25%. In general, both accuracy and linearity of the curved-bladed system deteriorated slightly as the flow speed increased. This may be a result of the wake-dependent fluctuations of the flow pattern in the vicinity of the curved-bladed rotor with increasing flow speed.

In the range 10–100 cm s<sup>-1</sup>, the accuracy of the flat-bladed system varied from -2.50% to -0.87%. Beyond 100 cm s<sup>-1</sup>, the accuracy of this system varied from -2.0% to +1.94%. In the range 10–100 cm s<sup>-1</sup>, the flat-bladed meter's linearity varied from 0% to -1.33%. Beyond 100 cm s<sup>-1</sup>, its linearity varied from +1.89% to -2.66%.

The observed fluctuations in accuracy and linearity with increasing flow speed are attributable to the formation of Karman vortices behind the cylindrical rotor-supporting hardware located in front of the rotor, and their break off with increasing Reynolds number *Re* of the flow. As *Re* increases, with flow speed, there are marked changes in the pattern of flow behind a cylinder, with the formation of "circulation" and a pair of vortices behind the cylinder as *Re* approaches 20. As *Re* exceeds 40, a complete change in character of flow takes place with the vortices getting longer and finally breaking off, and traveling downstream with the fluid. The fluid then curls around behind the cylinder and makes a new vortex. Subsequently, the vortices peel off alternately on each side forming a "Karman vortex street." When this happens the velocity at any point behind the cylinder varies with time. As the value of *Re* increases to several hundred, the vorticity begins to fill in a thin band behind the cylinder where the flow is chaotic and irregular. With further increase in *Re* the thickness of this band increases and the flow begins to twist and turn in all three dimensions (Feynman et al. 1964). The Reynolds number for our configuration went up  $3 \times 10^4$  for a flow velocity of 300 cm s<sup>-1</sup>, and the changes in flow pattern in the vicinity of the Savonius rotor as described are likely to have contributed

to the observed fluctuations of accuracy and linearity of the meter with increasing flow speed.

Although the flat-bladed rotor meter was simpler in construction, and was devoid of a frame and related attachments, this flowmeter exhibited flow accuracy and linearity characteristics poorer than that of a curved-bladed rotor meter.

#### a. Influence of support rods on the meter's azimuth response

Since the Savonius rotor needs to be held within the supporting hardware of the instrument, flow obstructions from them tend to modify the flow pattern in the vicinity of the rotor and, therefore, affect its response to the flow field. If the flowmeter is held in a normal attitude, flow modifications by the supporting plates at the bottom and top of the rotor tend to remain the same irrespective of changes in directions of the incident flow. However, if the vertically held meter is rotated in azimuth, for the same incident flow, the flow experienced by the rotor will change as the heading of the supporting rods situated outside the rotor's periphery changes. This will introduce some errors in the meter's flow output as it is rotated in the azimuth.

In contrast to a fixed-vane system, the body of a free-vane system does not have a fixed orientation with respect to the flow direction. Consequently, for the same incident flow, the flow pattern in the volume cell swept by the rotor of a free-vane system can vary during the measurement interval, resulting in corresponding variations in the Savonius rotor's directional sensitivity in the horizontal plane. Flow pattern modifications imposed by the two support rods of the free-vane system have been calculated using the formula (Eskinazi 1965)

$$V = (V_r^2 + V_\theta^2)^{1/2},$$

where *V* is flow at any given point in the volume cell swept by the rotor blades, under the influence of a given rod; *V<sub>r</sub>* is the flow component along the line joining a given point and the axis of the given rod; and *V<sub>θ</sub>* is the flow component at this point perpendicular to *V<sub>r</sub>*. Here, *V<sub>r</sub>* and *V<sub>θ</sub>* are given by

$$V_r = U_0 \left[ \left( \frac{a_0}{r} \right)^2 - 1 \right] \cos \theta \quad (1)$$

$$V_\theta = U_0 \left[ \left( \frac{a_0}{r} \right)^2 + 1 \right] \sin \theta, \quad (2)$$

where *U<sub>0</sub>* is undisturbed flow approaching the cylindrical rod, *a<sub>0</sub>* is the radius of the rod, *r* is the distance between the axis of the rod and a given point, and *θ* is the angle between *r* and the vector *U<sub>0</sub>*. The formulas for *V<sub>r</sub>* and *V<sub>θ</sub>* are strictly valid only for rods of infinite length and when the flow is steady. However, these calculations enable first-order estimates to be made of

the flow patterns in the volume cell swept by the rotor blades.

The four cylindrical support rods (1-cm diameter) of the frame of the meter lay on a circle of 25-cm diameter. In the volume cell swept by the rotor blades, the average decrease in flow velocity due to the obstruction of flow by a pair of diametrically opposite rods of the frame, and flow enhancement by a pair of orthogonally located rods of this frame were approximately equal to 0.15% of the steady flow incident on the flowmeter. This implies that errors arising from the two mutually orthogonal pairs of rods of the frame essentially canceled out. The two internal rods (1-cm diameter) were closer to the rotor than the frame rods, and their influence on the flow pattern modifications in the volume cell swept by the curved blades of the rotor have been evaluated.

In the present case flow distribution in the volume cell swept by the rotor, under the influence of the two rods, was determined for an approaching flow  $U_0$  of  $100 \text{ cm s}^{-1}$ . The value of  $a_0$  was 1 cm. The results obtained in the cases of two mutually orthogonal orientations of flow with respect to the plane joining the

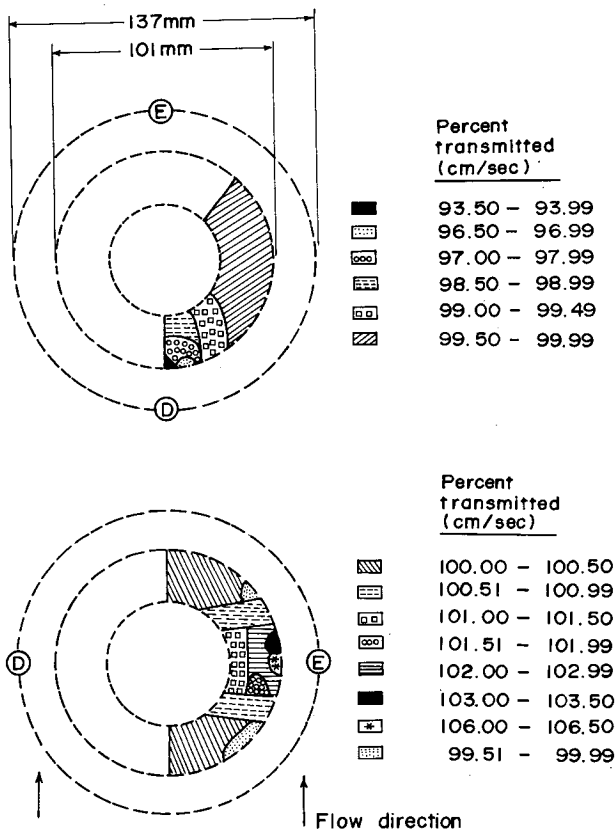


FIG. 6. Velocity distribution pattern in the volume cell swept by an Aanderaa curved-bladed Savonius rotor. The distribution, based on Eqs. (1) and (2) for an incident flow of  $100 \text{ cm s}^{-1}$ , represents idealized meter behavior. (a) Flow parallel to axis  $DE$  and (b) flow normal to axis  $DE$ .

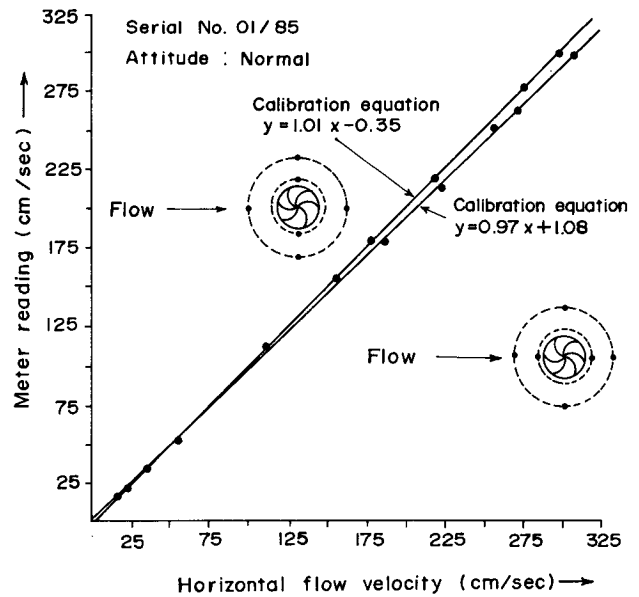


FIG. 7. Calibration limits in orthogonal flow orientations of the meter shown in Fig. 1a.

axes of the two support rods  $D$  and  $E$  are summarized in Figs. 6a and 6b, and allow the following observations to be made:

- (i) When the flow is parallel to the plane containing the axes of the two support rods, the effective flow experienced by the rotor is slightly less than the actual flow approaching the rotor.
- (ii) When the flow is normal to the plane containing the axes of the two support rods, the rotor experiences a slightly higher speed than actual.

Equations (1) and (2) suggest that the asymmetries in the flow patterns in the volume cell swept by the rotor in the two orientations shown in Figs. 6a and 6b can be reduced either by reducing the diameter of the support rods or by increasing the pitch circle of these rods.

Calibration of a "two-support rod" flowmeter, which employed an Aanderaa curved-bladed rotor, at the two orthogonal orientations of Fig. 6 yielded a more quantitative figure of the effective flow deviation. The results are summarized in Fig. 7. Beyond a towing speed of approximately  $75 \text{ cm s}^{-1}$  the flow output of the meter substantiates the theoretically deduced qualitative flow pattern observations of Figs. 6a and 6b. A difference of approximately  $2.5 \text{ cm s}^{-1}$  has been observed for the two orthogonal orientations at a towing speed of  $100 \text{ cm s}^{-1}$ . In the flow range  $25\text{--}75 \text{ cm s}^{-1}$  the difference in meter outputs at the two orthogonal orientations is negligible. Below a towing speed of  $25 \text{ cm s}^{-1}$ , the calibration result reveals a reversing trend. It appears that at small flow velocities some other effects that were not considered in the derivation of formulas (1) and (2) play a dominant role in modifying the flow in the vi-

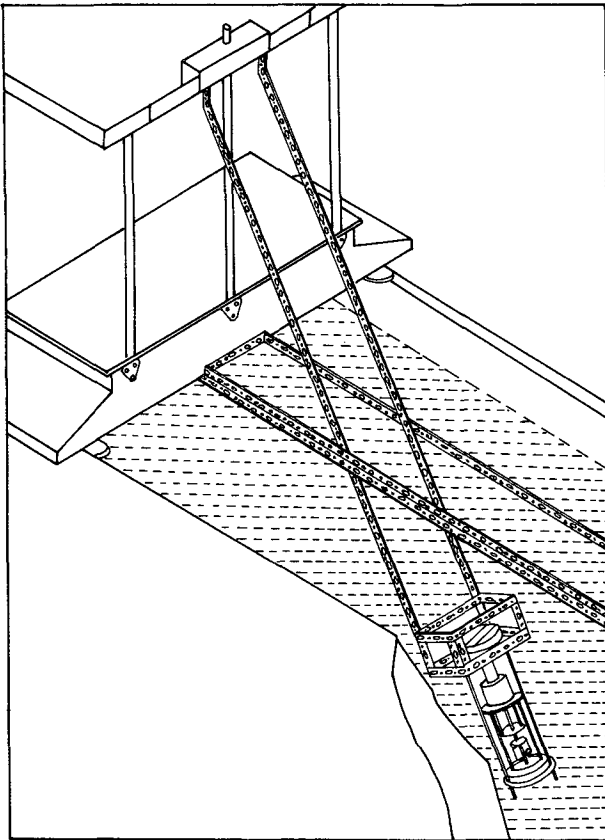


FIG. 8. Experimental setup for investigation of tilt response. In this figure, a meter shown in Fig. 1a is seen attached to the tilting mechanism.

city of the rotor. Because flow pattern variations at two limiting orientations have been considered, it is expected that the flow output of the meter at any other orientation will lie within the two orthogonal calibration limits. One method of reducing the directional

sensitivity of the rotor may be the use of a sufficiently large number of support rods instead of two. Detailed tow-tank experiments by Pite (1986) have shown that the flow asymmetries can be reduced to near zero if the number of support rods surrounding the flow sensor is such that near cancellation of positive and negative asymmetries occur.

*b. Tilt response*

The behavior of the two types of flowmeter's flow speed output while they are tilted from the vertical (i.e., their tilt response) has been investigated for some positive and negative tilt angles at various towing speeds. The experimental setup used for investigation of tilt response is shown in Fig. 8. Because the tilting mechanism used in the present investigation was held above the surface of water in the tow tank, it is likely that the tilting mechanism did not affect the flow in the vicinity of the rotor. Because all tests were performed on the current meter as it would be deployed in the field, with all hardware surrounding the rotor, the test results are expected to represent the total tilt performance characteristics of the meter rather than that of the rotor alone. The results are shown in Figs. 9a and 9b. Deviations from vertical cosine response at a given towing speed was derived as the difference between the measured flow output of the meter at  $\theta^\circ$  tilt from the vertical and the cosine of the flow output of the meter referenced to its normal attitude. For each towing speed of the meter in its tilted position, the expected flow output of the meter in its normal attitude has been derived from the least-squares fit of the flow calibration equation of the meter in its normal attitude.

The results revealed marked differences in the meter's tilt responses between positive and negative tilt angles. Similar observations were reported in the case of acoustic travel time difference and electromagnetic flow meters as well (Appell 1979). The observed nonlinearities in the tilt responses with increasing flow

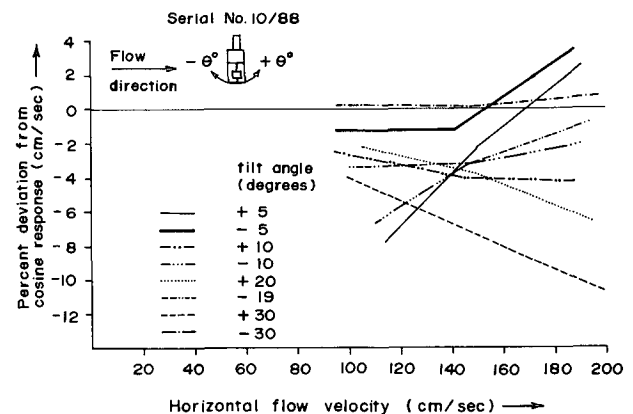
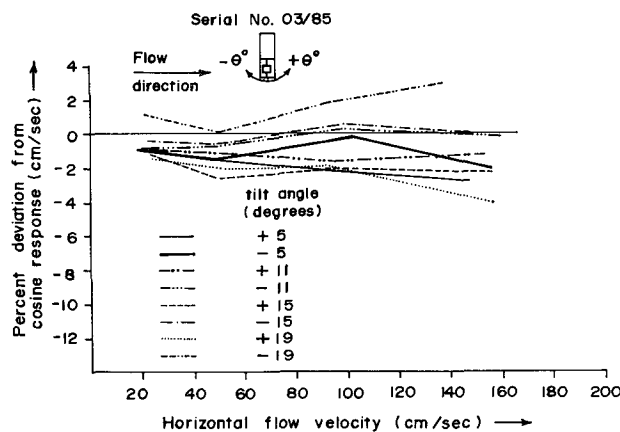


FIG. 9. (a) Tilt response of the flowmeter shown in Fig. 1a. (b) Tilt response of the flowmeter shown in Fig. 1b.

speed may be due to the speed-dependent wakes shed from the flowmeter's housing, and the resulting unsteady flows in the vicinity of the rotor. In unsteady flows the Savonius rotor may respond differently at different frequencies of the flow constituents. A similar inference was drawn by Karweit (1974), who conducted extensive laboratory tests of a Savonius rotor in oscillating flows of differing frequencies.

Examination of Fig. 9a reveals that the curved-bladed rotor meter's tilt responses had distinct trends in three ranges of speeds. While the deviations from cosine response generally increased gradually toward negative directions in the speed ranges from 20 to 50  $\text{cm s}^{-1}$  and 100 to 160  $\text{cm s}^{-1}$ , the deviations generally increased gradually toward positive direction in the speed range of 51–99  $\text{cm s}^{-1}$ . However, except in the speed range of 20–50  $\text{cm s}^{-1}$ , the responses at  $+5^\circ$  and  $+11^\circ$  exhibited the opposite trend. Figure 9b shows that, in general, the flat-bladed rotor meter (Fig. 1b) exhibited poorer cosine response for all positive tilt angles. A probable reason for this behavior may be the varying flow patterns, in the vicinity of the rotor for all positive tilt angles, that result from the eddy shedding and the flow reflecting from the meter parts. Because the rotor remained in the "zone of flow separation" of the flow-disturbing pressure case, reflections from the semicylindrical cover as well as the sensor characteristics become particularly important. Because the curved-bladed rotor flowmeter also had a similar pressure case, a major contribution for the observed deviations from cosine response in the case of the flat-bladed rotor meter can be attributed to the semicylindrical cover of the rotor assembly and the characteristics of the flat-bladed rotor. Nevertheless, the semicylindrical cover is a necessary component of the flat-bladed rotor system and, therefore, cannot be removed. For negative tilt angles, the flow obstructions as seen by the rotor were not as severe as in the case for positive tilt angles and, therefore, the tilt response was better than that for positive tilt angles.

### 5. Evaluation of flow direction performance

The direction calibration has been performed in the normal attitude of the flowmeter. A field far from local magnetic influences was selected as a simple and inexpensive calibration facility. Such a facility is adequate for calibration of direction (Appell et al. 1983).

For direction calibration of the fixed-vane system, a circle, whose diameter was equal to that of the base of the instrument, was drawn on a horizontal plane. This circle was divided into steps of  $10^\circ$ , starting from  $0^\circ$  (which coincided with the earth's magnetic north), as determined by an independent magnetic compass. The flowmeter was initially placed over the graduated circle on the horizontal plane so that the vertical plane passing through the axis of the fixed vane and that of the magnetic compass pointed toward  $0^\circ$ . The instru-

ment was operated as it is usually done in field measurements. After allowing a settling time of 30 s, the average of three successive readings, separated by an interval of 30 s, was recorded. The flowmeter was then slowly rotated clockwise so that the axis of its vane was positioned in line with the next graduation marking, separated by an angular spacing of  $10^\circ$ , and an average of three successive readings in this new position was recorded after allowing a settling time of 30 s. In this manner, readings over the entire range  $0^\circ$ – $360^\circ$ , in steps of  $10^\circ$ , were recorded, with the in-water unit rotated in the clockwise direction. Experiments were then repeated in the same manner with the in-water unit rotated in the counterclockwise direction.

In the case of the free-vane system, a graduated protractor glued to the base plate located below the free vane served as a reference for direction orientation of the vane. Because the vane was free to rotate about the axis of the instrument, rotation of the instrument was not performed. The experiment was initiated after pointing the "zero" of the protractor to the earth's magnetic north, as determined by an independent magnetic compass. An experiment was conducted by pointing the vertical plane of symmetry of the wedge-shaped free vane to successive graduations on the protractor, at angular intervals of  $10^\circ$ . An average of three successive readings was recorded for each position of the vane, during its clockwise and counterclockwise rotations.

The least-squares-fitted calibration equation for stepwise rotation of the in-water unit of the fixed-vane meter in the clockwise and counterclockwise directions in steps of  $10^\circ$  revealed a hysteresis of approximately  $6^\circ$  in the entire range of  $0^\circ$ – $360^\circ$  (see Fig. 10a). The observed hysteresis of this system must be solely due to the inherent hysteresis of the magnetic compass used in the present investigation. Visual observations of the movements of the magnet assembly, inside the magnetic compass, during its gentle and violent rotations indicated that both sticking frictional effects at the bearings and damping due to the oil in the compass contributed to the observed hysteresis. An additional hysteresis of approximately  $5^\circ$  in the case of the free-vane system (Fig. 10b) arose from the poor coupling between its vane and the circular potentiometer of the direction-sensing assembly. The direction errors of the free-vane system over the full-scale range were within  $-2.5\%$  and  $+6.1\%$  of the full scale. The observed errors included those of the magnetic compass, the circular potentiometer, and those arising from its hysteresis during clockwise and counterclockwise rotations of the vane. The fixed-vane system exhibited better accuracy. For this system the errors were within  $-2.2\%$  and  $+1.66\%$  of the full scale. The deviations from linearity of the free-vane system's direction output over the full-scale range, inclusive of hysteresis, lay within  $-2.5\%$  and  $+3.36\%$ . The fixed-vane system exhibited better linearities compared to the free-vane system. The lin-



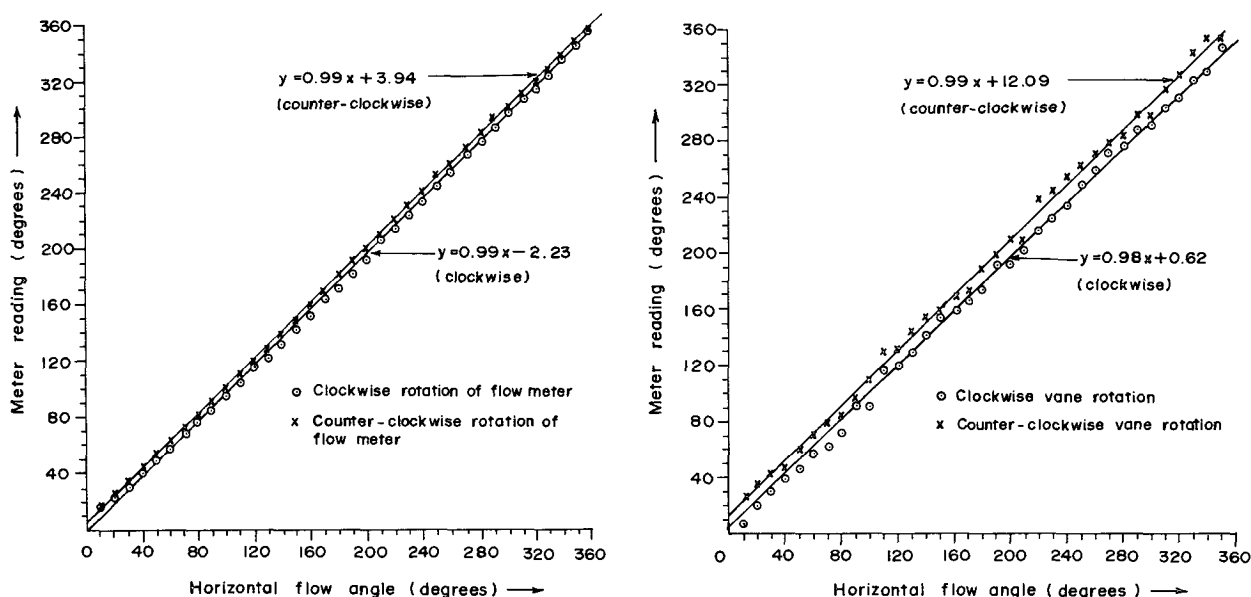


FIG. 10. (a) Hysteresis effect of fixed-vane flowmeter of Fig. 1b. (b) Hysteresis effect of free-vane flowmeter of Fig. 1a.

erarity deviations of the fixed-vane system lay within  $-1.16\%$  and  $+1.5\%$ .

## 6. Conclusions

The results of the present investigations can be summarized as follows. A “two-support rods” configuration for a curved-bladed rotor is not suitable for a free-vane system of flowmeter. A fixed-vane flowmeter exhibits superior direction performance compared to a free-vane flowmeter. The comparatively poor direction performance of the free-vane system is due to the poor coupling to the “vane-follower” magnet from the external vane. Compared to a curved-bladed rotor the flat-bladed rotor assembly is particularly sensitive to tilt. Its large and inconsistent deviations from cosine response have been attributed to the flow distortions caused by the semicircular cover of the rotor assembly.

*Acknowledgments.* We are thankful to D. Rodrigues, V. N. Chodankar, E. D’Silva, A. Shirgaonkar, and Mrs. V. Damodaran, who provided technical assistance in the fabrication of the instruments. Assistance from R. Y. P. Desai and the technical staff of CWPRS during the tow-tank experiments is gratefully acknowledged. We are also grateful to the referees of this journal who provided useful suggestions for the improvement of the original manuscript. This work was partly funded by Calcutta Port Trust.

## REFERENCES

- Appell, G. F., 1979: Performance assessment of advanced ocean current sensors. *IEEE J. Oceanic Eng.*, 4, 1–4.
- , K. A. Mooney, and W. E. Woodward, 1983: A framework for the laboratory testing of Eulerian current measuring devices. *IEEE J. Oceanic Eng.*, 8, 2–8.
- Dean, J. P., 1985: Problems and procedures associated with the calibration of ocean current sensors. Vol. 4, *Advances in Underwater Technology and Offshore Engineering*, Graham & Trotman Ltd., 83–101.
- Doebelin, E. O., 1983: Generalised performance characteristics of instruments. *Measurement Systems, Application and Design*, McGraw-Hill, 37–206.
- Eskinazi, S., 1965: Uniform flow around a cylinder. *Principles of Fluid Mechanics*, Allyn and Bacon Inc., 286–290.
- Feynman, R. P., R. B. Leighton, and M. Sands, 1964: The flow of wet water. Vol. 2, *Lectures on Physics*, Addison-Wesley, 41–1 to 41–12.
- Joseph, A., 1987: A technique for display applications. *Electron. Eng.*, 59, 27.
- , and E. Desa, 1992: Laboratory performance evaluation of some Savonius rotor type current meters of differing mechanical designs. NIO Tech. Rep. No. NIO/TR-3/92. [Available from the Publication and Reprography Division, National Institute of Oceanography, P.O. NIO, Dona Paula, Goa-403004, India.]
- , and —, D. Rodrigues, E. J. D’sa, and R. Y. P. Desai, 1986: Design of a microcomputer based flow measuring instrument. Vol. 2, *Proc. Third Indian Conf. on Ocean Engineering*, Bombay, India, Indian Institute of Technology, 73–84.
- Karweit, M., 1974: Response of a Savonius rotor to unsteady flow. *J. Mar. Res.*, 32, 359–364.
- Pite, H. D., 1986: The influence of support rods on the rotation speed of Savonius rotors. *J. Atmos. Oceanic Technol.*, 3, 487–493.